IOP Publishing Semiconductor Science and Technology
Semicond. Sci. Technol. 32 (2017) 025014 (8pp) doi:10.1088/1361-6641/32/2/025014

A theoretical study of the optical Stark effect in InGaAs/InAlAs quantum dots

Dinh Nhu Thao[1,2], Le Thi Ngoc Bao[2], Duong Dinh Phuoc[2] and Nguyen Hong Quang[3,4]

[1] Duy Tan University, K7/25 Quang Trung Street, Danang City, Vietnam
[2] College of Education, Hue University, 34 Le Loi Street, Hue City, Vietnam
[3] Institute of Physics, Vietnam Academy of Science and Technology, 18 Hoang Quoc Viet Street, Hanoi, Vietnam
[4] Institute for Scientific Information, Vietnam Academy of Science and Technology, 18 Hoang Quoc Viet Street, Hanoi, Vietnam

E-mail: dnthao@dhsphue.edu.vn

Received 2 August 2016, revised 10 November 2016
Accepted for publication 11 November 2016
Published 19 January 2017

Abstract

In this paper, we examine the three-level optical Stark effect of excitons in InGaAs/InAlAs quantum dots using renormalized wavefunction formulation. The system was assumed to be irradiated by two lasers in which a strong laser dynamically couples electron-quantized levels, while a weaker laser probes interband absorption. Our results show that, in the presence of the resonant strong laser, two new absorption peaks of excitons appear in the absorption spectrum as a clear indication of the effect. In addition, we propose that the formation of the effect in low-dimensional structures could have connection to the splitting of electron levels. Furthermore, we seek to explain the essential dependence of the amplitude and position of two peaks on pump field detuning.

Keywords: optical Stark effect, quantum dots, exciton resonance, InGaAs, InAlAs

(Some figures may appear in colour only in the online journal)

1. Introduction

Semiconductor low-dimensional structures have become more appealing to the scientific community in recent decades due to their extraordinary electronic, optical, thermal, and mechanical properties compared to their bulk counterparts [1–5]. The advantages of these structures include high surface areas and possession of quantum size effects, which yield surface effects and discrete energy spectra as well as confined wave functions of electrons and holes [4, 5]. Such structures can be applied to the production of devices, e.g., laser diodes [6–8], photodectectors [9, 10], THz emitters [11–13], field-effect transistors [14, 15], energy storage, and high-performance conversions [16, 17]. In these structures, quantum dots (QDs) exhibit more promising properties and applications than higher-dimensional structures such as quantum wells [18–20].

The optical Stark effect of excitons in low-dimensional structures was first discovered in semiconductor quantum wells in 1986 [21], and has been studied extensively since then [22–26]. This effect has considerably transformed the absorption spectra of excitons and therefore has made significant change to applications such as creating a new optical switching. The optical Stark effect in quantum wells is classified into two groups, including two-level and three-level Stark effects. While the former is a light-induced effect [27], the latter is the result of coupling of two excited states [28]. Moreover, since the three-level Stark effect requires lower-intensity laser sources of much lower photon energy in interband transitions, it occurs more readily and is more applicable than the two-level counterpart. Characterization of the three-level Stark effect in quantum wells can be performed using the theory of three-level nonlinear susceptibility [24] or by a renormalized wavefunction formulation [28]. The renormalization method is shown to provide a clearer view inside the effect.

Recently, there have been several experimental projects related to the optical Stark effect in semiconductor QDs

[29–33]. These works emphasized future devices of quantum computation such as ultrafast all-optical switching, hybrid phototransistors, and entangled photon pairs. Interestingly, the characteristics of the devices were found to be significantly affected by the optical Stark effect. However, there has been no extensive theoretical study on the three-level optical Stark effect in semiconductor QDs. Hence, it is imperative to investigate how the effect influences semiconductor QDs due to relevant interests in basic physics as well as optimization of devices.

Nanostructures made from $In_{0.53}Ga_{0.47}As/In_{0.52}Al_{0.48}As$ layers were reported to have advantages such as large conduction-band discontinuity, about 500 meV [34], which can be treated as an infinite barrier for the electrons in these structures. Furthermore, these structures can be doped with Si atoms more readily so as to raise the densities of electron gas. They can also be used in ultralow-loss fiber communications systems due to their short-wavelength infrared working range at 2–4 μm [34].

In this paper, we monitor the three-level optical Stark effect of excitons in $In_{0.53}Ga_{0.47}As/In_{0.52}Al_{0.48}As$ QDs in renormalized wavefunction formulation as for quantum wells. Sections 2 and 3 are devoted to the formulation of the basic equations and the analysis of three-level optical Stark effect in the QDs. Section 4 summarizes our approach and presents key results.

2. Model and theory

2.1. Model

We use isotropic, direct band gap, parabolic two-band semiconductors. QDs are assumed to be spherical, with an infinite potential barrier that confines all particles inside (see page 5 of [35] and ref [36]). Those assumptions would simplify analytical calculations without undermining the model's reliability, and would be especially suitable to small dots with large band offsets. Consider a QD confined in an infinite spherical potential well $U(r)$ with the dot radius R such as

$$U(r) = \begin{cases} 0 & \text{if } r \leqslant R \\ \infty & \text{if } r > R, \end{cases} \tag{1}$$

where r is the magnitude of the position vector of the electron from the dot center. The total wavefunction of electrons and holes are given as

$$\Psi(\vec{r}) = u_{c,v}(\vec{r})\Psi^{e,h}(\vec{r}), \tag{2}$$

where $u_{c,v}(\vec{r})$ is the periodic Bloch function located near the center of the Brillouin zone, with c and v signifying the conduction and valence band, respectively. The envelope wavefunction of the electrons and holes in the spherical coordinates is given as follows (see pages 11–15 in reference [35]):

$$\Psi^{e,h}(\vec{r}) = \Psi^{e,h}(r, \theta, \phi) = Y_{lm}(\theta, \phi) f_{nl}(r), \tag{3}$$

where n, l, m are quantum numbers and $Y_{lm}(\theta, \phi)$ is the spherical harmonic function. The normalized radial part of this wave function is

$$f_{nl}(r) = \sqrt{\frac{2}{R^3}} \frac{j_l\left(\chi_{nl}\frac{r}{R}\right)}{j_{l+1}(\chi_{nl})}, \tag{4}$$

where $j_l(r)$ is the spherical Bessel function and χ_{nl} is its zero-points. The corresponding energies of electron and hole are determined respectively by

$$E^e_{nl} = E_g + \frac{\hbar^2\chi^2_{nl}}{2m_e R^2}, \tag{5}$$

and

$$E^h_{nl} = \frac{\hbar^2\chi^2_{nl}}{2m_h R^2}, \tag{6}$$

where m_e, m_h are the effective masses of electron and hole in bulk semiconductor, and E_g is the bandgap of the semiconductor.

Then we compute the interaction Hamiltonian between the electron and the electromagnetic field. The pump and probe lasers can be described by

$$\vec{E}(t) = \vec{n}A_x e^{-i\omega_x t}, \tag{7}$$

where A_x, ω_x are the magnitude and frequency of the laser wave, respectively; x represents pump or probe laser. Using a radiation gauge with $div\vec{A} = 0$ and $\Phi = 0$ (see page 117 of [35], and also ref [37]) we are able to determine vector potential to be

$$\vec{A} = \vec{A}_x(t) = \vec{n}\frac{A_x}{i\omega_x}e^{-i\omega_x t}. \tag{8}$$

When the electromagnetic field is not so strong that we can omit higher-order terms, and Coulomb gauge is applied, the electron–electromagnetic field interaction Hamiltonian can be written as [37, 38]

$$H_{\text{int}} = -\frac{e}{m_0}\hat{\vec{p}} \cdot \vec{A}, \tag{9}$$

where e, m_0, and $\vec{p}$ are the charge, bare mass, and momentum of the electron, respectively. Substituting equation (8) into (9), we have

$$H_{\text{int}} = -\frac{e}{m_0}\frac{A_x e^{-i\omega_x t}}{i\omega_x}\vec{n} \cdot \hat{\vec{p}}. \tag{10}$$

The matrix element for an optical transition from the initial state $|i\rangle$ to the final state $|f\rangle$, in the presence of the just-discussed laser, is then determine by

$$v_{fi} = \langle f|H_{\text{int}}|i\rangle, \tag{11}$$

where

$$\begin{cases} |i\rangle = u_i(\vec{r})\Psi^{e,h}_i(\vec{r}) \\ |f\rangle = u_f(\vec{r})\Psi^{e,h}_f(\vec{r}) \end{cases}. \tag{12}$$

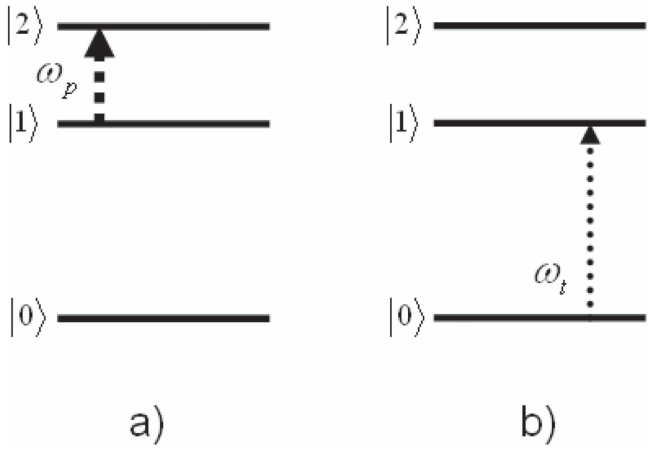

Figure 1. The three-level model: $|0\rangle$ is the level of hole, $|1\rangle$ and $|2\rangle$ are the electron levels. Optical transition by: (a) pump laser photon ω_p between $|1\rangle$ and $|2\rangle$, denoted by a thick dashed arrow; (b) probe laser photon ω_t between $|0\rangle$ and $|1\rangle$, denoted by a thin dashed arrow.

2.2. Matrix element for optical transition between electron levels

In order to investigate optical transitions in QDs, we need the transition rates or the absorption probabilities in a unit of time, which can be calculated using Fermi's golden rule. We therefore have to work with the matrix element for optical transition that appears in the formula of Fermi's golden rule. In the three-level model, the lowest level corresponds to the first quantized state of the hole in the valence band, while the other two levels are associated with the lowest quantized states of electrons in the conduction band (figure 1). Therefore, in order to investigate the three-level optical Stark effect, we need to consider both the intersubband transition between electron levels of a strong pump laser and the interband transition between two lowest levels of hole and electron of a probe laser. When both lasers operate simultaneously, the strong pump laser provides a mixing state with renormalized wavefunction, while the probe counterpart yields the three-level optical Stark effect.

We first calculate matrix element for the optical intersubband transition between electron levels $|1\rangle$ and $|2\rangle$ under the effect of a pump laser denoted by a thick dashed arrow in figure 1(a). The two corresponding states are then described by the total wavefunctions with the same Bloch function $u_c(\vec{r})$, and the initial state and the final state are determined by

$$\begin{cases} |1\rangle = u_c(\vec{r})\Psi^e_{1s}(\vec{r}) \\ |2\rangle = u_c(\vec{r})\Psi^e_{1p}(\vec{r}) \end{cases}. \tag{13}$$

As mentioned in the previous section, pump laser is assumed to be

$$\vec{A}_p(t) = \vec{n}\frac{A_p}{i\omega_p}e^{-i\omega_p t}, \tag{14}$$

where A_p is the magnitude of pump wave. Combining equations (10) and (14) then substituting into equation (11), we have the matrix element for an intersubband transition between two electron quantized levels of $1s$ and $1p$

$$v_{21} = -\frac{e}{m_0}\frac{A_p e^{-i\omega_p t}}{i\omega_p}\langle\Psi^e_{1p}(\vec{r})|\vec{n}.\,\hat{\vec{p}}|\,\Psi^e_{1s}(\vec{r})\rangle. \tag{15}$$

In order to calculate the optical transition rates, we will need the momentum matrix element between the band states, which was given as follows for the intersubband transition

$$\langle\Psi^e_2(\vec{r})|\vec{n}.\,\hat{\vec{p}}|\,\Psi^e_1(\vec{r})\rangle = -\frac{m_e}{i\hbar}(E^e_{1p} - E^e_{1s}) \times \langle\Psi^e_{1p}(\vec{r})|\vec{n}.\,\vec{r}|\,\Psi^e_{1s}(\vec{r})\rangle. \tag{16}$$

Supposing the polarization of the light is parallel to the z-axis, we have

$$v_{21} = V_{21}e^{-i\omega_p t}, \tag{17}$$

where

$$V_{21} = \frac{eA_p}{\hbar\omega_p}\frac{m_e}{m_0}\frac{2R}{i\sqrt{3}}\frac{(E^e_{1p} - E^e_{1s})}{j_1(\chi_{1s})j_2(\chi_{1p})} \times \int_0^R j_0(\chi_{1s}r)j_1(\chi_{1p}r)r^3dr. \tag{18}$$

Similar calculations would yield an equation system

$$\begin{cases} V_{12} = V^*_{21} \\ V_{11} = V_{22} = 0, \end{cases} \tag{19}$$

where V^*_{21} is the complex conjugate of V_{21}.

2.3. Exciton absorption in the absence of the pump laser

We will find the matrix element for optical transition between the two lowest levels of hole and electron $|0\rangle$ and $|1\rangle$ or exciton absorption under the effect of a probe laser in the absence of the pump laser, as depicted by a thin dashed arrow in figure 1(b). It is an interband transition, so two corresponding states are described by the total wavefunctions with the different Bloch function. Hence, the initial state and final states are determined by

$$\begin{cases} |0\rangle = u_v(\vec{r})\Psi^h_{1s}(\vec{r}) \\ |1\rangle = u_c(\vec{r})\Psi^e_{1s}(\vec{r}) \end{cases}. \tag{20}$$

As mentioned in the previous section, probe laser is assumed to be

$$\vec{A}_t(t) = \vec{n}\frac{A_t}{i\omega_t}e^{-i\omega_t t}. \tag{21}$$

Therefore, combining equations (10) and (21) and then substituting into equation (11), we can deduce the matrix element for an interband transition between two quantized levels of $1s-$state of electron and hole as follows

$$T_{10} = -\frac{eA_t}{i\omega_t}\frac{p_{cv}}{m_0}e^{\frac{i}{\hbar}(E^e_{1s} - E^h_{1s} - \hbar\omega_t)t}, \tag{22}$$

where p_{cv} is the polarization matrix element between conduction and valence band. From that we can deduce the

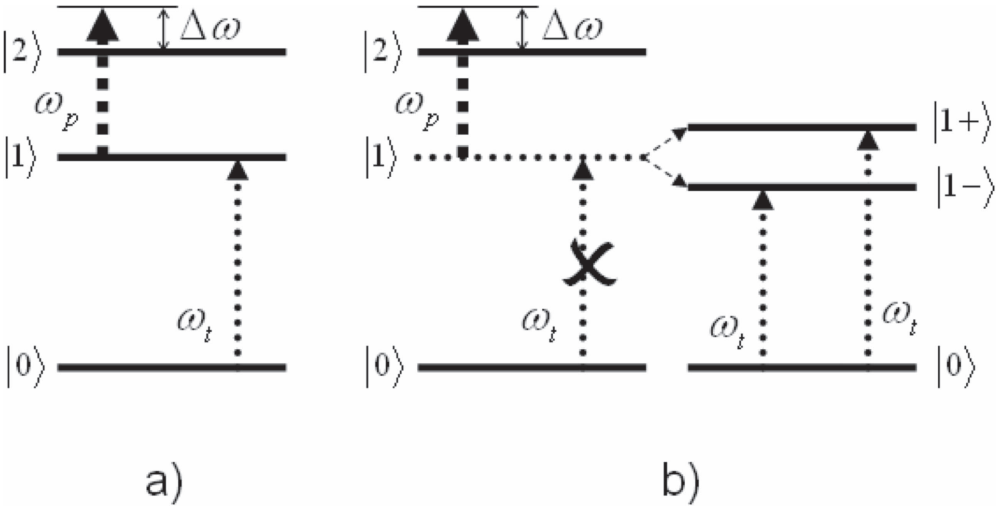

Figure 2. Three-level model in the simultaneous presence of a pump and probe laser: (a) optical transitions are expected to be observed as usual; (b) scenario is revealed from calculation. Vertical dashed arrows mean the same as in figure 1. $|1+\rangle$ and $|1-\rangle$ are the splitting levels of the first level of electrons after the pump laser is turned on.

transition rate under the effect of a probe laser [39]

$$W_0 = \frac{2\pi}{\hbar}\left(\frac{eA_t}{\omega_t}\frac{p_{cv}}{m_0}\right)^2 \delta(E_{1s}^e - E_{1s}^h - \hbar\omega_t). \tag{23}$$

We then apply the well-known 'Lorentz line' function [40] to calculate the approximated form of the transition rate

$$W_0 = B\frac{\Gamma}{(E_g^{dot} - \hbar\omega_t)^2 + \Gamma^2}, \tag{24}$$

where Γ is the phenomenological linewidth of absorption peak; note that we use a monochrome probe laser; $E_g^{dot} = E_{1s}^e - E_{1s}^h$, and

$$B = \frac{2}{\hbar}\left(\frac{eA_t}{\omega_t}\frac{p_{cv}}{m_0}\right)^2. \tag{25}$$

2.4. Exciton absorption in the presence of the pump laser

We find the absorption spectra of the excitons by irradiating a probe laser in the presence of a pump laser whose frequency is nearly equal to the energy difference between two electron levels (figure 2). In order to observe the three-level optical Stark effect in the QDs, some conditions must be satisfied. Firstly, the pump laser intensity must be significantly stronger than the probe laser. Secondly, the detuning of the pump laser to the electron levels must be much smaller than the frequency of the pump laser and band gap of active material in QDs

$$\Delta\omega \ll \omega_p \ll E_g/\hbar. \tag{26}$$

In the presence of a pump laser, the wavefunction of the electron is renormalized as

$$\Phi_{mix}^e(\vec{r}, t) = \sum_n c_n(t) e^{-\frac{i}{\hbar}E_n t}\,|n\rangle, \tag{27}$$

where $|n\rangle = \Psi_n^e(\vec{r})$ $(n = 1, 2)$ are stationary wavefunctions of electrons and E_n are the energy eigenvalues before the time $t = 0$ at which the pump laser starts to operate. Here

$$\begin{cases} c_1(t) = \dfrac{1}{2\Omega}(\alpha_1 e^{i\alpha_2 t} + \alpha_2 e^{-i\alpha_1 t}) \\ c_2(t) = -\dfrac{V_{21}}{2\Omega\hbar}(e^{i\alpha_1 t} - e^{-i\alpha_2 t}) \end{cases}, \tag{28}$$

where $\hbar\omega_{21} = E_2 - E_1 = E_{1p}^e - E_{1s}^e$ and

$$\begin{cases} \alpha_1 = \Omega - \dfrac{\Delta\omega}{2} \\ \alpha_2 = \Omega + \dfrac{\Delta\omega}{2} \end{cases}, \tag{29}$$

as well as

$$\begin{cases} \Omega = \sqrt{\left(\dfrac{\Delta\omega}{2}\right)^2 + \dfrac{|V_{12}|^2}{\hbar^2}} \\ \Delta\omega = \omega_p - \omega_{21} \end{cases}. \tag{30}$$

V_{12} is the matrix element of the intersubband transition between the $n = 1$ and $n = 2$ sublevels of electrons under the action of the pump wave, as presented in section 2.1, equation (18). V_{12} is a function of radius of QD, and thus is different from the cases of bulk semiconductor and quantum wells that are independent of the size of the considered structures.

The matrix element corresponding to this transition between 1 *s*-state of hole and the coupling (mixed) state of electrons under the effect of the probe laser is given as

$$T_{mix,o} = \frac{eA_t}{i\omega_t}\frac{p_{cv}}{m_0}\left(\frac{1}{2\Omega}(\alpha_1 e^{i\alpha_2 t} + \alpha_2 e^{-i\alpha_1 t})\right)^* \times e^{\frac{i}{\hbar}(E_g^{dot} - \hbar\omega_t)t}\langle\Psi_{1s(mix)}^e(\vec{r})|\,\Psi_{1s}^h(\vec{r})\rangle, \tag{31}$$

where $\Psi_{1s(mix)}^e(\vec{r})$ is the renormalized electron wavefunction of the first level. Then we can find the transition rate as

follows [39]

$$W = \frac{2\pi}{\hbar}\left(\frac{eA_t}{\omega_t}\frac{p_{cv}}{m_0}\right)^2\left[\left(\frac{\alpha_1}{2\Omega}\right)^2\delta(E_g^{dot} - \hbar\omega_t - \hbar\alpha_2) + \left(\frac{\alpha_2}{2\Omega}\right)^2\delta(E_g^{dot} - \hbar\omega_t + \hbar\alpha_1)\right]. \quad (32)$$

Here, we omit the crossing terms due to the small contribution to the spectrum resulting from the least overlap of the delta functions. Performing a similar procedure as in the previous section, we get the approximated form of the transition rate [40]

$$W = B\left[\left(\frac{\alpha_1}{2\Omega}\right)^2\frac{\Gamma}{(E_g^{dot} - \hbar\omega_t - \hbar\alpha_2)^2 + \Gamma^2} + \left(\frac{\alpha_2}{2\Omega}\right)^2\frac{\Gamma}{(E_g^{dot} - \hbar\omega_t + \hbar\alpha_1)^2 + \Gamma^2}\right], \quad (33)$$

where $\Gamma \to 0$ is the phenomenological linewidth as mentioned before. As illustrated in equation (33), the transition rate depends directly on many parameters of the system: effective masses of electron and hole, polarized parameter, detuning between pump laser and two electron quantized energy levels, QD size, intensity of pump laser, as well as profile of absorption peak, etc. From equation (33), we can expect that there will be two exciton peaks in the absorption spectra as a result of the indeterminate form of two terms of this equation. The schematic diagram of possible excitations is presented in figure 2(b), while figure 2(a) shows the schematic diagram of usual optical transitions. Both original electron levels are split under the strong electric field of a pump wave. Using equations (27) to (30), we can determine the splitting levels of the first original level of electron, corresponding to states $|1+\rangle$ and $|1-\rangle$, as

$$\begin{cases} E_1^+ = E_1 + \hbar\alpha_1 \\ E_1^- = E_1 - \hbar\alpha_2 \end{cases}. \quad (34)$$

Furthermore, the splitting levels of the second original level of electron, corresponding to states $|2+\rangle$ and $|2-\rangle$, are given by

$$\begin{cases} E_2^+ = E_2 + \hbar\alpha_2 \\ E_2^- = E_2 - \hbar\alpha_1 \end{cases}. \quad (35)$$

Moreover, the conservation of the energy-level average between the original states and the shifting and splitting states

$$\frac{E_1^+ + E_1^-}{2} = E_1 - \frac{\hbar\Delta\omega}{2}, \quad (36)$$

or

$$\frac{E_2^+ + E_2^-}{2} = E_2 + \frac{\hbar\Delta\omega}{2}, \quad (37)$$

can be deduced from equations (34) and (35). However, the splitting levels of the second original level of electron E_2^+ and E_2^- were omitted from the diagram in figure 2(b) since the selection rule for the interband transition in QDs limits the contribution of these levels to the optical Stark effect. Detailed explanations for the splitting of electron levels and formation of the three-level optical Stark effect are given in the next section.

3. Results and discussion

Now we apply our theory to consider the three-level optical Stark effect of excitons in $In_{0.53}Ga_{0.47}As/In_{0.52}Al_{0.48}As$ QDs. The parameters used in the calculation are as follows. The effective mass of electron and hole in the dot material $In_{0.53}Ga_{0.47}As$ are $m_e = 0.042m_0$ and $m_h = 0.052m_0$; the band gap of the dot material is $E_g = 750$ meV; the pump laser amplitude is $A_p = 4 \times 10^4$ V/cm; and the linewidth is $\Gamma = 0.1$ meV. A high-conduction band offset, which is about 500 meV, could serve as infinite potential for the electrons moving in the dot.

We first examine the exciton absorption spectra to seek the existence of the three-level optical Stark effect of excitons. We begin with a simple case of a spherical QD with radius 60 Å and zero pump field detuning (figure 3). The dashed line and solid line represent two cases under consideration: in the absence and in the presence of the pump laser, respectively. When the pump laser is absent, starting from equation (24), we observe one original absorption peak only (the dashed line), which signifies the transition between the two lowest quantized energy levels of electron and hole. This observation could be explained by the selection rule for the interband transition. However, after irradiating a strong pump laser, which is resonant with two quantized levels of electrons, there appear two peaks of excitons in the absorption spectra as expected from equation (33). These two peaks are located symmetrically on both sides of the original peak (solid line, figure 3). Interestingly, the shifting and splitting of spectral peaks of excitons in the presence of a strong optical wave are similar to those of spectral lines in an external electric field seen in the Stark effect. In other words, the results provide clear evidence of the existence of the three-level optical Stark effect in this quantum structure, quite similar to the effect in quantum well structures [21–26].

In order to investigate further this effect, we first consider the influence of the pump field detuning on the peak profile. The exciton absorption spectra in spherical QDs is rendered with radius $R = 60$ Å, and in the presence of the pump laser with detuning $\Delta\omega = 0$ meV (thin solid line), $\Delta\omega = 0.1$ meV (thick solid line), and $\Delta\omega = 0.3$ meV (dashed line) (figure 4). In all cases, we observe two peaks of excitons in the absorption spectra, though with different peak height. Therefore, this observation also confirms the existence of the three-level optical Stark effect.

It is really exciting to explore the origin of the effect. The mechanism of this effect can be understood from the scheme depicted in figure 2(b). Under a strong pump laser which is resonant with two quantized levels of an electron, the lowest state of the electron is renormalized and split into two sublevels, one being higher and another being lower compared to the original level in the energy scale, obeying the energy conservation. Therefore, when we probe the exciton, we do

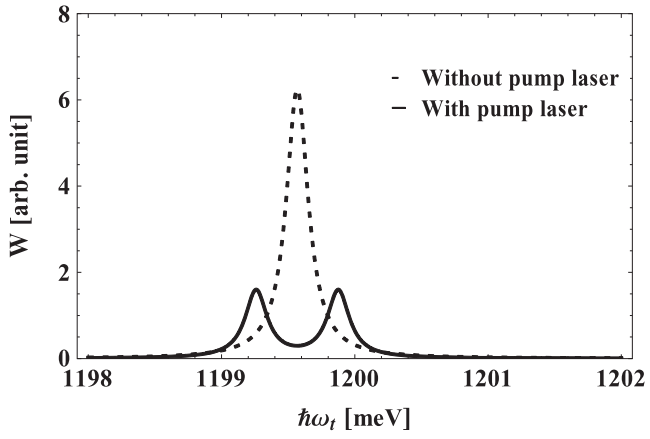

Figure 3. The exciton absorption spectra in spherical QDs with radius $R = 60$ Å in the absence (dashed line) and presence (solid line) of pump laser with pump field detuning $\Delta\omega = 0$ meV.

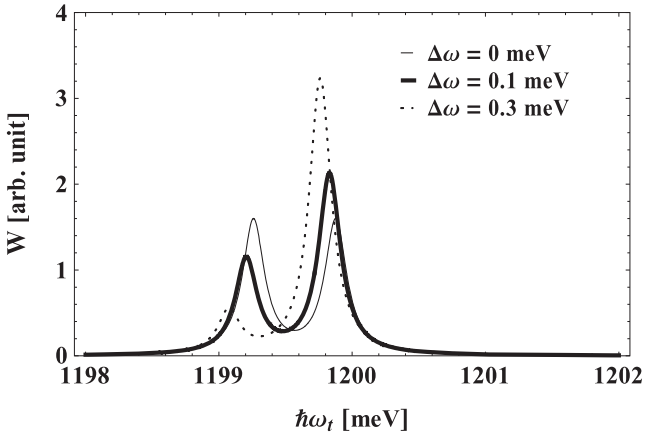

Figure 4. Exciton absorption spectra in spherical QDs with radius $R = 60$ Å in the presence of the pump laser with three different detunings $\Delta\omega = 0$, 0.1, and 0.3 meV.

not see the original absorption peak. Instead, we notice two new transitions from the hole level to these two renormalized electron levels. Consequently, two new exciton peaks were observed. This effect can be utilized to build an ultrafast switching for future optical equipment. More specifically, by turning on a strong laser, we can shift the absorption spectra states back and forth between complete absorption and transparency in femtoseconds.

However, there has been no precedent study that explains the reasons why the first electron level splits under a strong pump laser and leads to the formation of the three-level optical Stark effect in low-dimensional structures. Therefore, collective results from this study provide us more insights into this phenomenon. This splitting resembles the one happening during the Stark effect, except that it requires the existence of a strong pump laser that is resonant with two quantized levels of electrons in QDs. This strong resonant laser plays a role as a 'connection' between the two quantized levels of electrons. Consequently, the strong laser creates a two-fold big level whose linewidth is equal to the energy difference of the two levels. Then, under the strong electric field of a pump wave, the symmetry of this degeneracy level is broken as in the

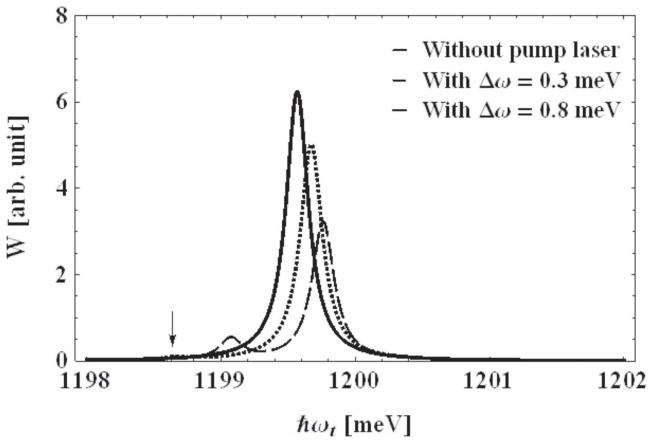

Figure 5. Exciton absorption spectra in spherical QDs with radius $R = 60$ Å in the absence (solid line) and presence of pump laser with pump field detuning $\Delta\omega = 0.3$ (dashed line) and 0.8 (dotted line) meV.

Stark effect. Consequently, both original electron levels are split. We, however, notice only two exciton peaks corresponding to transitions among the hole level and two splitting levels of the first original electron level, which agrees with the selection rule for the interband transition in QDs. And due to low-dimensional structures possessing similar discrete band diagrams, we would expect that this explanation is also applicable to other structures such as quantum wells.

It is interesting that figure 4 also reveals the characteristics of peaks and the conservation of the transition rate. The amplitude and position of these two peaks depend quite essentially on the detuning between the pump laser and two electron levels. When the detuning increases, one of the peaks heightens but the other shrinks. Hence, larger amplitude difference between two peaks is observed with significant detuning magnitude. This dependence can be explained by assuming that, in the absence of the pump laser (figure 3), there is only one peak with the highest height and with a finite transition rate R. This rate is fixed for a specific transition in a certain low-dimensional structure due to the rate being determined by certain parameters of the density of states and the square of the electric dipole matrix element [41]. When the pump laser is turned on, due to the symmetry of the two splitting levels, two peaks share the same transition rate and therefore the same height. The total transition rate is fixed so that each transition rate of these two peaks should be equivalent with one half of R. These two symmetric peaks with the same height, located at the both sides of the original peak, are obtained in the presence of the pump laser with the zero detuning. Figure 5 illustrates the exciton absorption spectra states when the detuning increases, encompassing the spectra in the absence of the pump laser and in the presence of the pump laser with large detunings $\Delta\omega = 0.3$ and $\Delta\omega = 0.8$ meV. We observe that, at larger detuning, one of the two splitting peaks tends to recover back the original peak while the other deviates from it. The former yields a higher transition rate and therefore a higher height and larger linewidth than those of the latter. More specifically, the former's

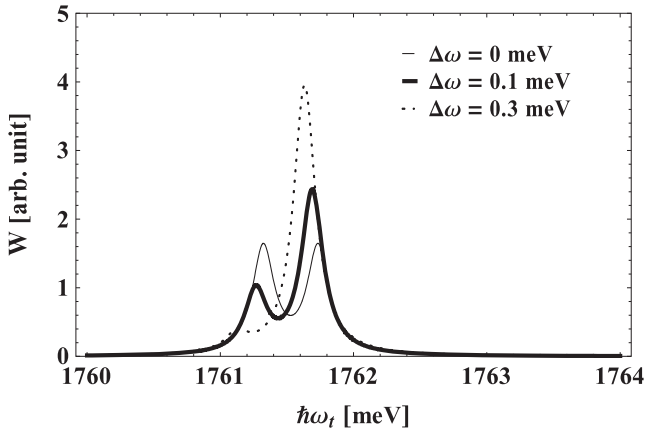

Figure 6. Same as figure 4 but with radius $R = 40$ Å.

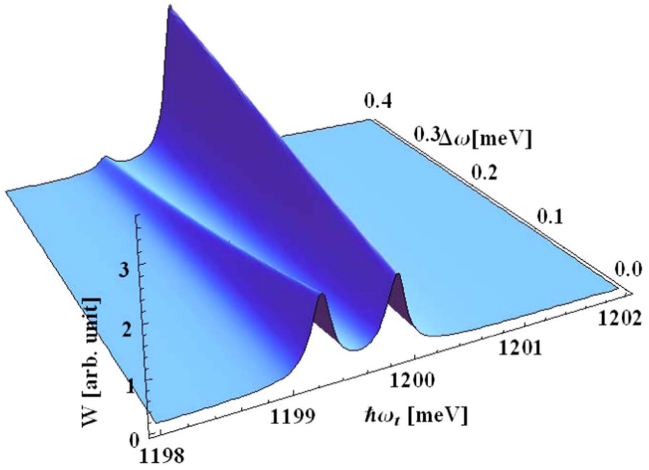

Figure 7. Exciton absorption spectra in spherical QDs in the presence of pump laser with radius $R = 60$ Å as a function of detuning $\Delta\omega$ and photon energy $\hbar\omega_t$.

height is equal to ~50% and 80% of the original peak height at $\Delta\omega = 0.3$ meV and $\Delta\omega = 0.8$ meV, respectively. In other words, the former's height is an increasing function of the detuning. In addition, the linewidth of the big splitting peak is larger than the original peak's counterpart and reduces to the original peak's linewidth when the detuning reaches a very large magnitude.

Moreover, this dependence is stronger as the dot radius is smaller, as can be seen in figures 4 and 6. With the same detuning of 0.3 meV, the height of the low-energy peak changes according to the dot radius. The low-energy peak still exists when the dot radius is 60 Å (figure 4) but nearly disappears when the dot radius is as small as 40 Å (figure 6). Furthermore, when the detuning varies, the peak positions also vary accordingly.

These phenomena can be seen more clearly in figure 7, in which the changes are made continuously. When the detuning goes from 0 to 0.4 meV, one peak tends to zero while the other emerges gradually. However, both peaks shift in the same direction. We can see that the amplitude and position of the two peaks depends monotonously on the detuning.

4. Conclusions

In this paper, we explore the existence and characteristics of the three-level optical Stark effect of excitons in InGaAs/InAlAs QDs using renormalized wavefunction formulation. Our results show that, when the pump wave is turned on, two new absorption peaks of excitons appear as clear evidence of the existence of the effect. The amplitude and position of these two absorption peaks depend essentially on the detuning magnitude between the pump laser and two electron-quantized energy levels. These dependences are stronger with smaller dot radius. In addition, an explanation for the formation of the effect in low-dimensional structures is clearly presented in connection with the splitting of electron levels due to the presence of the strong pump field. Furthermore, we explain the reasons why the electron levels are split, why only the first electron level contributes to the effect, and why large detuning leads to a large difference in amplitude of the two exciton peaks. For simplicity, in this work we consider spherical QDs but this assumption is not expected to undermine the model's reliability. We hope that future research projects will seek to verify our theory with related experimental results. We also hope to expand our theory to quantum beats, a similar and important problem in low-dimensional structures.

Acknowledgments

We would like to thank Dr Ly Quoc Dung, Brunel University, UK for giving many useful comments and Oanh Vu, Vanderbilt University, USA for her assistance in manuscript preparation. This research is funded by the Vietnam National Foundation for Science and Technology Development (NAFOSTED) under grant number 103.01-2014.46.

References

[1] Yoffe A D 1993 *Adv. Phys.* **42** 173
[2] Balandin A 2000 *Phys. Low-Dimens. Struct.* **1** 1
[3] Tien N T, Thao D N, Thao P T B and Quang D N 2016 *J. Appl. Phys.* **119** 214304
[4] Barnham K and Vvedensky D 2008 *Low-Dimensional Semiconductor Structures: Fundamentals and Device Applications* 1st edn (Cambridge: Cambridge University Press) ch 6–9, pp 180–325
[5] Weisbuch C and Vinter B 2014 *Quantum Semiconductor Structures: Fundamentals and Applications* 1st edn (Boston: Academic Press, Inc.) ch 2–5, pp 11–141
[6] Nakamura S, Senoh M, Nagahama S I, Iwasa N, Yamada T, Matsushita T, Kiyoku H and Sugimoto Y 1996 *Jpn. J. Appl. Phys.* **35** L74
[7] Nakamura S, Senoh M, Nagahama S, Iwasa N, Yamada T, Matsushita T, Sugimoto Y and Kiyoku H 1997 *Appl. Phys. Lett.* **70** 868
[8] Newell T C, Bossert D J, Stintz A, Fuchs B, Malloy K J and Lester L F 1999 *IEEE Photon. Technol. Lett.* **11** 1527
[9] Peng L, Hu L and Fang X 2013 *Adv. Mater.* **25** 5321
[10] Zheng W, Huang F, Zheng R and Wu H 2015 *Adv. Mater.* **27** 3921

[11] Otsuji T, Watanabe T, Tombet S A B, Satou A, Knap W M, Popov V V, Ryzhii M and Ryzhii V 2013 *IEEE Trans. Terahz. Sci. Technol.* **3** 63
[12] Thao D N, Katayama S and Tomizawa K 2004 *J. Phys. Soc. Jpn.* **73** 3177
[13] Thao D N and The N P 2013 *J. Phys. Soc. Jpn.* **82** 104701
[14] Dey A W, Svensson J, Ek M, Lind E, Thelander C and Wernersson L 2013 *Nano Lett.* **13** 5919
[15] Pregl S, Weber W M, Nozaki D, Kunstmann J, Baraban L, Opitz J, Mikolajick T and Cuniberti G 2013 *Nano Res.* **6** 381
[16] Peng K, Wang X, Li L, Hu Y and Lee S 2013 *Nano Today* **8** 75
[17] Weng B, Liu S, Tang Z and Xu Y 2014 *RSC Adv.* **4** 12685
[18] Tighineanu P, Daveau R S, Lehmann T B, Beere H E, Ritchie D A, Lodahl P and Stobbe S 2016 *Phys. Rev. Lett.* **116** 163604
[19] Cao G *et al* 2016 *Phys. Rev. Lett.* **116** 086801
[20] Delbecq M R *et al* 2016 *Phys. Rev. Lett.* **116** 046802
[21] Mysyrowicz A, Hulin D, Antonetti A, Migus A, Masselink W T and Morkoç H 1986 *Phys. Rev. Lett.* **56** 2748
[22] Schmitt-Rink S and Chemla D S 1986 *Phys. Rev. Lett.* **57** 2752
[23] Lehmen A V, Chemla D S, Zucker J E and Heritage J P 1986 *Opt. Lett.* **11** 609
[24] Fröhlich D, Wille R, Schlapp W and Weimann G 1987 *Phys. Rev. Lett.* **59** 1748
[25] Quang N H and Bobrysheva A I 1993 *Phys. Scr.* **47** 121
[26] Quang N H 1993 *Int. J. Mod. Phys.* B **07** 3405
[27] Combescot M 1992 *Phys. Rep.* **221** 167
[28] Garmire E, Maradudin A A and Rebane K K (ed) 1991 *Laser Optics of Condensed Matter* 1st edn vol 2 (New York: Plenum) p 369
[29] Biswas C, Jeong H, Jeong M S, Yu W J, Pribat D and Lee Y H 2013 *Adv. Funct. Mater.* **23** 3653
[30] Bose R, Sridharan D, Solomon G S and Waks E 2011 *Appl. Phys. Lett.* **98** 121109
[31] Gall C L, Brunetti A, Boukari H and Besombes L 2011 *Phys. Rev. Lett.* **107** 057401
[32] Unold T, Mueller K, Lienau C, Elsaesser T and Wieck A D 2004 *Phys. Rev. Lett.* **92** 157401
[33] Vasa P, Wang W, Pomraenke R, Maiuri M, Manzoni C, Cerullo G and Lienau C 2015 *Phys. Rev. Lett.* **114** 036802
[34] Asai H and Kawamura Y 1991 *Phys. Rev.* B **43** 4748
[35] Bányai L and Koch S W 1993 *Semiconductor Quantum Dots* 1st edn (Singapore: World Scientific) ch 1
[36] Çakır B, Yakar Y, Özmen A, Sezer M Ö and Şahin M 2010 *Superlattices Microstruct.* **47** 556
[37] Band Y B 2006 *Light and Matter: Electromagnetism, Optics, Spectroscopy and Lasers* 1st edn (New York: Wiley) ch 5, p 296
[38] Jorio A, Dresselhaus M S, Saito R and Dresselhaus G 2011 *Raman Spectroscopy in Graphene Related Systems* (New York: Wiley) ebook, Part 1, ch 5, Sec. 5.4.1
[39] Schwabl F 2007 *Quantum Mechanics* 4th edn (Berlin-Heidelberg: Springer) ch 16, p 296
[40] Balakrishnan V 2003 *Resonance* **8** 48
[41] Fox M 2001 *Optical Properties of Solids* 1st edn (Oxford: Oxford University Press) ch 6, p 125